1. Studies on Hull Form Design by Means of Nonlinear Programming

Kazuo SUZUKI*, *Member*

(*From J.S.N.A. Japan, Vol. 145, June 1979, Vol. 150, Dec. 1981, Vol. 151, June 1982, Vol. 153, June 1983, Vol. 154, Dec. 1983 and Vol. 158, Dec. 1985*)

Summary

The hull form design can be regarded as a kind of the problem of nonlinear programming , because the objective function is generally specified as the nonlinear functional of the hull form and many constraints of equality or inequality types are needed in the practical design stage. In the present state, however, the nonlinear programming is commonly used in the field of structural design, in spite of its flexibility and possibility in practical applications to almost all engineering problems. In this paper, the author discusses the hull form design based on the wave resistance theory by means of the nonlinear programming.

Two types of the problem are studied as examples of the hull form design. One is the determination of the best curve of sectional area under several side conditions, in which a wall–sided ship is assumed. The other problem is the improvement of a given hull form with practical frame lines in order to reduce the total resistance. It is shown by numerical examples and experimental verifications that the nonlinear programming technique provides a rational method for the design of good hull forms.

1. Introduction

Hull form design methods based on the wave resistance theory have been discussed by many reseachers and designers, and the least resistance hull forms under the given design conditions have been pursued. In these studies the variational approach played a doninant role as the scheme to minimize the objective function of each problem. However the application of the variational method is very difficult for the cases including nonquadratic objective functions and/or nonlinear side conditions. Especially, if the problem contains the constraints of inequality type, the variational approach is of no use. For these cases, the nonlinear programming becoms very effective to solve the problem. The technique is commonly used in the field of structural design nowadays, but it has flexibility and possibility in practical applications to almost all engineering problems including design work. In this paper, the author applies the nonlinear programming to the problem of hull form design based on the wave resistance theory, employing SUMT (Sequential Unconstrained Minimization Technique)[1) as the scheme of nonlinear programming.

Two types of the problem are discussed ,one of which is the minimum wave resistance problem of wall–sided ships, and the other is the problem of hull form improvement of practical ships. The result of the former problem will serve as design data of sectional area curve at the initial design stage. In the latter problem, lines of the fore body of a given hull form are improved so as to make the total resistance minimum under various constraints of practical importance. In both cases, the thin ship theory and the low speed theory are used as the evaluation formula of wave making resistance.

2. Nonlinear Programming : SUMT

In the optimization process, the objective functions shown in subsequent sections are minimized under the prescribed design constraints by means of the nonlinear program-

* Faculty of Engineering, Yokohama National University

ming technique.Now we will discuss the optimization scheme used in the present study briefly.

The formal expression of an optimization problem is described as follows.

"Minimize the objective function $I(\boldsymbol{x})$ subject to constraints expressed by inequalities $C_i(\boldsymbol{x})>0$, i=1, 2,......, N."

In our problem, $I(\boldsymbol{x})$ means wave (or total) resistance or otherwise an equivalent functional defined later, and $\boldsymbol{x}$ is the vector representation of design variables defining the hull surface or hull form characteristics. Both geometrical constraints and practical design constraints about the hull form are included in $C_i(\boldsymbol{x})$. For the purpose of the numerical treatment of these constraints, we can apply the sequential unconstrained minimization technique abbreviated as SUMT, which is well known as one of the internal penalty techniques. In case of SUMT, the above problem is transformed as follows.[1]

"Minimize the modified objective function

$$F(\boldsymbol{x}, r_k)=I(\boldsymbol{x})+r_k\sum_{i=1}^{N}\{1/C_i(\boldsymbol{x})\},\ r_k>0 \quad (2.1)$$

without constraints for a monotonically decreasing sequence values (perturbation parameters) r_k, $k=1, 2, ..., K$."

In the present computation, the modified objective function is minimized by Zangwill's direct search method[2] without calculating derivatives. This combined algorithm with SUMT and Zangwill's direct search is very powerful, because SUMT has the advantage that the inequality constraints are added in a comparatively easy way and Zangwill's method is stable for any nonlinearities. Zangwill's direct search is constructed and executed by the systematized one directional searches based on the quadratic interpolation.

3. Minimum Wave Resistance Preblem of Wall-sided Ships

3.1 Statement of the Problem

The minimum wave resistance problem for wall–sided ships has been investigated by means of the variational approach so far,[3)4)5)6)] and the theory of wave resistance employed in this problem has been limited to Michell's thin ship theory. The same kind problem can be extended to full hull forms by means of the nonlinear programming applied to the low speed theory. The common statements of these problems about minimum wave resistance are described in this section, namely the formulations are discussed with respect to the objective function and constraints.

In this paper, the right hand co–ordinate system with positive x toward the bow, y athwart ships, and z positive downwards is taken. The origin of the co–ordinates is placed on the still water plane at the midship. We assume the elementary ship with wall–sided main hull of draught T whose waterline shape is expressed by the equation $y=f(x)$, because the wave making characteristic is principally governed by the form of the sectional area curve. Now the following normalized expressions are employed,

$$x=l\xi \quad , \quad f(x)=1/2\cdot\bar{B}\varphi(\xi) \qquad (3.1)$$

where l is the half length $L/2$ and $\bar{B}$ is the mean breadth of a ship such as

$$\bar{B}=\frac{1}{l}\int_{-l}^{l}f(x)\,dx. \qquad (3.2)$$

The condition of constant displacement is obtained from eqs. (3.1) and (3.2), namely

$$D_c=\int_{-1}^{1}\varphi(\xi)\,d\xi=2. \qquad (3.3)$$

Generally speaking this kind of the problem has been formulated in such a way that the wave resistance is minimized under the constraint (3.3). But the numerical results based on such formulation yield undesirable shapes,for example, the waterline curves have unfair parts or the hull forms at the both ends show extreme swan neck forms. In order to eliminate these undesirable shapes, we need to introduce the fairness condition of the hull form in the present formulation. It may be desired in general that the fairness criterion is defined from the hydrodynamic point of view, however it is defined as an artificial functional for simplicity in the present work. In the field of curve fairing problem,the following functional is employed as the fairness criterion in many cases.

$$F_c=\int_{-1}^{1}\left(\frac{d^2\varphi}{d\xi^2}\right)^2 d\xi \tag{3.4}$$

In this study, however, the fairness criterion is defined by a slightly different form, which is shown in the next section, but has to be equivalent to eq. (3.4) by its meaning.

According to the above–mentioned considerations, fundamental aspects of the problem are stated in such a way that the wave resistance should be minimized under constraints such as constant displacement, suitable fairness and so forth. We define the wave resistance coefficient $C_w{}^*=\pi R_w/\rho U^2\bar{B}^2$, where R_w being wave resistance, ρ being fluid density and U being ship speed. Then one can express $C_w{}^*$ in the form like.

$$\left.\begin{aligned} C_w{}^*=&\int_0^{\pi/2}(\{p^*(\theta)\}^2\\ &+\{q^*(\theta)\}^2)\sec^3\theta\, d\theta. \end{aligned}\right\} \tag{3.5}$$

Amplitude functions $p^*(\theta)$, $q^*(\theta)$ are given in later sections, and have different representations according to respective wave resistance theory. Two formulations can be considered with regard to the treatment of fairing constraint.

(1) Objective Function

$I=C_w{}^*$

Constraints

$D_c=2,\ F_c<\alpha$ etc.

(2) Objective Function

$I=C_w{}^*+\beta F_c$

Constraints

$D_c=2$ etc.

Parameters α and β are concerned with the degree of fairness, which are determined from the practical point of view. Numerical examples shown in later sections are mainly based on the method (2),because the method (1) needs more computer time than that of the method (2) from the strict constraint $F_c<\alpha$.

3.2 Approximation of Wall-sided Ship and Treatment of Constraints

In the optimization process based on SUMT, high speed computations are needed with respect to the objective function and the constraints, because the modified objective function must be evaluated many times according to the gradual shape deformation. In the present problem square stations (S.S.)are expressed as $\xi=\xi_i\,(i=-I,\ \ldots\ldots,\ -1,0,1,\ \ldots\ldots,\ I)$ with $\xi_{-I}=-1,\ \xi_0=0,\ \xi_I=1$ and $|\xi_i|=|\xi_{-i}|$, and the waterline of the wall–sided ship is approximated by the polygonal line with straight line segments on $\xi_i\leqq\xi\leqq\xi_{i+1}$. We can select each ordinates $\varphi(\xi_i)=\varphi_i$ as the design variables. If the coefficient of fineness C_p is given in the problem, φ_0 is excluded from the design variables on account of $\varphi_0=1/C_p$ in our formulation. According to this approximation, many numerical treatments in the optimization can be carried out in easy way.

The expression of D_c in eq. (3.3) is obtained as follows by the present approximation,

$$D_c=\sum_{i=-I}^{I} c_i\,\varphi_i \tag{3.6}$$

where c_i is a constant determined from the formula of numerical integration. The condition $D_c=2$ can be satisfied by use of the following technique. When the condition of constant displacement is broken as

$$\sum_{i=-I}^{I} c_i\,\varphi_i=2\delta \neq 2 \tag{3.7}$$

by the shape deformation, each ordinate is renewed as φ_i/δ to keep $D_c=2$. If the coefficient of fineness is fixed in the problem, this modification is replaced as $(1-c_0\varphi_0)\varphi_i/(\delta-c_0\varphi_0)$.

The fairness criterion is defined as follows instead of eq. (3.4) in this place,

$$\left.\begin{aligned} F_c=&2\left(\frac{\varphi_1-\varphi_0}{\xi_1-\xi_0}\right)^2+2\left(\frac{\varphi_0-\varphi_{-1}}{\xi_0-\xi_{-1}}\right)^2\\ &+\left(\sum_{i=-I+1}^{-1}+\sum_{i=1}^{I-1}\right)\cdot \end{aligned}\right\} \tag{3.8}$$

$$\left(\frac{\varphi_{i+1}-\varphi_i}{\xi_{i+1}-\xi_i}-\frac{\varphi_i-\varphi_{i-1}}{\xi_i-\xi_{i-1}}\right)^2 \quad \rfloor$$

As we discussed in the previous section, eq. (3.8)have a meaning equivalent to eq. (3.4).

The other constraints of inequality type are needed in order to obtain reasonable shapes. These are specified as

$$\left.\begin{array}{ll} \varphi_i \geqq 0 & (i=-I, \ldots\ldots, 0, \ldots\ldots, I) \\ \varphi_i \geqq \varphi_{i+1} & (i=0, \ldots\ldots, I-1) \\ \varphi_i \geqq \varphi_{i-1} & (i=-I+1, \ldots\ldots, 0) \end{array}\right\} \quad (3.9)$$

all of which are added in both formulations (1) and (2) stated in the previous section.

Under the above-mentioned preparations, the optimization can be executed, however we need the wall-sided ship to start the computation of nonlinear programming. In this paper, the initial hull form is defined by

$$\varphi(\xi)=\frac{3}{2}(1-\xi^2) \quad (3.10)$$

in the ordinary case, and

$$\left.\begin{array}{l} \varphi(\xi)=\dfrac{12-15\,C_p}{2\,C_p}(1-\xi^2) \\ \quad +\dfrac{-10+15\,C_p}{2\,C_p}(1-\xi^4) \end{array}\right\} \quad (3.11)$$

in the case that the coefficient of fineness is fixed.

3.3 Numerical Examples

3.3.1 Application of the Thin Ship Theory

As the first example of this work, Michell's thin ship theory is applied; if we take the end shape effect into consideration,the amplitude functions in eq. (3.5) can be written as follows,

$$\left.\begin{array}{l} \left.\begin{array}{l} p^*(\theta) \\ q^*(\theta) \end{array}\right\} = -\cos^2\theta\,(1-e^{-\gamma_0 t\,sec^2\theta})\cdot \\ \quad \left\{ \displaystyle\int_{-1}^{1} \frac{d\varphi}{d\xi} \begin{array}{c}\cos\\ \sin\end{array} (\gamma_0 \xi\, sec\,\theta)\, d\xi \right. \\ \quad -\varphi(1) \begin{array}{c}\cos\\ \sin\end{array} (\gamma_0\, sec\,\theta) \\ \quad \left. +\varphi(-1) \begin{array}{c}\cos\\ \sin\end{array} (-\gamma_0\, sec\,\theta) \right\} \\ \quad \mp \dfrac{1}{2}\mu_f \gamma_0{}^2\, sec\,\theta\, e^{-\gamma_0 \zeta_f\, sec^2\theta} \cdot \\ \qquad \begin{array}{c}\sin\\ \cos\end{array} (\gamma_0 \xi_f\, sec\,\theta) \\ \quad \mp \dfrac{1}{2}\mu_a \gamma_0{}^2\, sec\,\theta\, e^{-\gamma_0 \zeta_a\, sec^2\theta} \cdot \\ \qquad \begin{array}{c}\sin\\ \cos\end{array} (\gamma_0 \xi_a\, sec\,\theta) \end{array}\right\} \quad (3.12)$$

where $t=T/l$, $\gamma_0=gl/U^2=1/2\,Fn^2$ and U is the ship speed. An integral term in right hand side of eq. (3.12) means the wave making effect of the main hull based on the thin ship theory. If $\varphi(1)$ and $\varphi(-1)$ are non-zero and included in the design variables, they correspond to the bluff end shapes. In addition, the effect of bulbous bow and stern can be represented by immersed point doublets at (ξ_f, 0, ζ_f) and (ξ_a, 0, ζ_a). Their intensities μ_f and μ_a correspond to bulb sizes.

In the first place, symmetric hull forms with normal end shapes are optimized. As examples shown in Fig. 1, swan neck forms near both ends are almost suppressed and optimum coefficients of fineness agree well to the results obtained by the variational method.[4] In practical design problems,however, there are many cases where the coefficient of fineness is specified. Examples of the optimum hull forms with prescribed prismatic coefficients are shown in the form of sectional area curves in Fig. 2. In Fig. 3 the optimum hull forms with normal or bluff end shapes are compared with the results of optimum doublet distributions obtained by the variational method, which correspond to shapes with cylindrical endings.[4]

In the next place ,symmetric hull forms with bulbous bow and stern are examined, in which not only the bulb sizes but also the bulb positions are taken as design variables. In such cases that the bulb position is taken as design

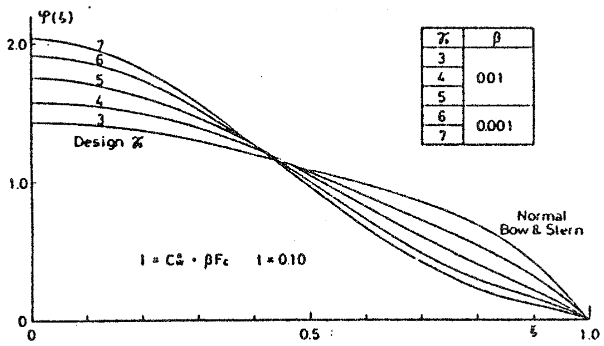

Fig. 1 Optimum hull forms with normal bow and stern

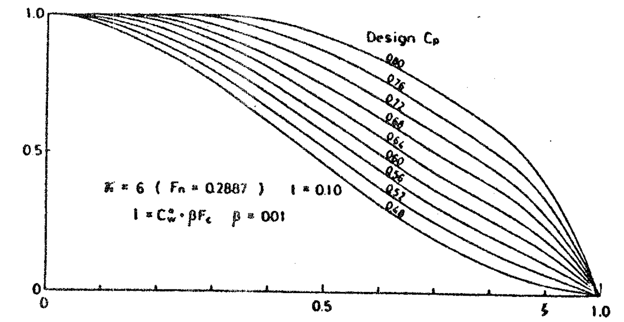

Fig. 2 Optimum hull forms with prescribed prismatic coefficient

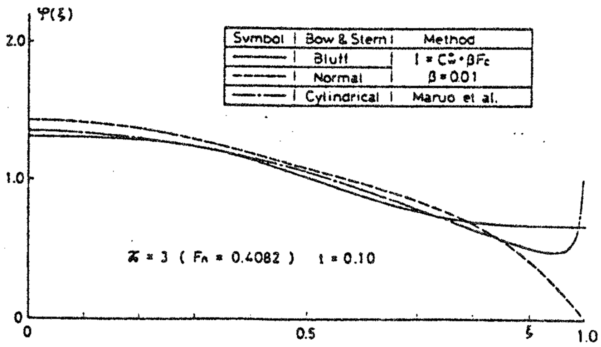

Fig. 3 Comparison of optimum hull forms

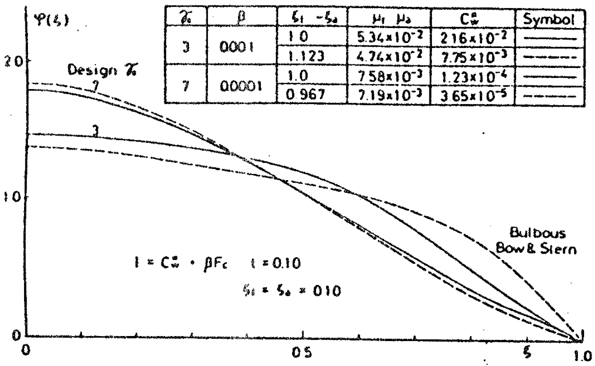

Fig. 4 Optimum hull forms with bulbous bow and stern

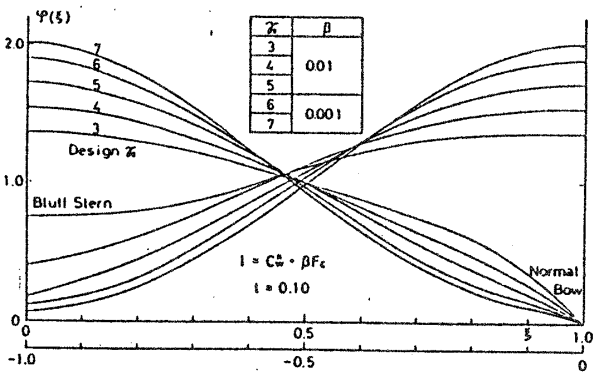

Fig. 5 Optimum hull forms with normal bow and bluff stern

variables, the variational method is not applicable, since the objective function becomes highly nonlinear. Examples of this case are compared with those having bulbs in fixed positions as in Fig. 4. Differences between both cases are remarkable.

Final examples shown in Fig. 5 are asymmetric hull forms having normal bow and bluff stern, whereas the preceding examples are symmetric. Optimizations about other asymmetric cases, which have bulbous bow and normal or bluff stern, can be carried out in similar way as given in the reference 7).

3.3.2 Application of the Low Speed Theory

It is well known that there are several methods to predict wave making resistance of hull forms to which the thin ship theory is not applicable. Among them, the low speed theory proposed by Baba et al.[8] and Maruo[9] is based on the perturbation from the double model flow. This theory has no restrictions in the hull geometry such as thin or slender, while it seems to be suitable in moderate or low speed range from the theoretical background.

Now the application of the low speed theory is described in place of the thin ship theory. In the present study, the simplified formula given by Maruo[10] is employed in order to reduce the

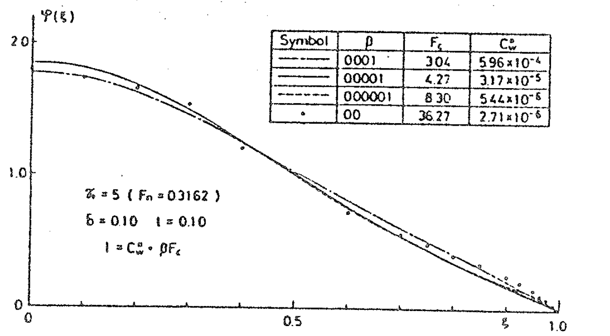

Fig. 6 Optimum hull forms with and without fairing constraint

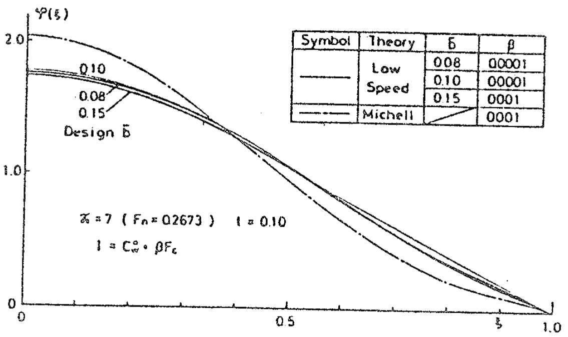

Fig. 7 Comparison of optimum hull forms

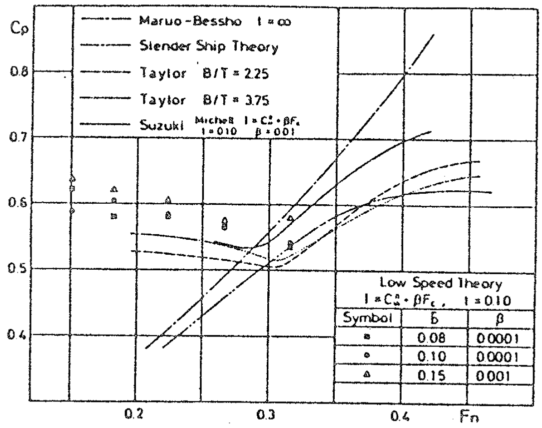

Fig. 8 Comparison of optimum coefficient of fineness

computer time ; the amplitude functions in eq. (3.5) are expressed as follows in case of the wall–sided hull form,

$$
\left.\begin{array}{l} p^*(\theta) \\ q^*(\theta) \end{array}\right\} = \mp \frac{\cos\theta}{2\gamma_0}\int_{-1}^{1} \frac{d\chi}{d\xi}\,\frac{d\varphi}{d\xi}\,\begin{array}{c}\sin\\ \cos\end{array}(\gamma_0 \xi \sec\theta)\cdot \cos(\gamma_0 \bar{b}\varphi(\xi)\sec\theta\tan\theta)\,d\xi \tag{3.13}
$$

where $\bar{b}=\bar{B}/L$ and

$$
\chi(\xi)=u_0(u_0^2+v_0^2-1). \tag{3.14}
$$

As shown in eq. (3.13), the effect of finite breadth of a ship is considered. In eq. (3.14), u_0 and v_0 are fluid velocities normalized by U around the double model in x and y directions respectively, in which the uniform flow component is included. Integrating eq. (3.13)by parts, the following expressions without the derivative of $\chi(\xi)$ are obtained.

$$
\left.\begin{array}{l} p^*(\theta) \\ q^*(\theta) \end{array}\right\} = \frac{1}{2}\int_{-1}^{1}\chi(\xi)\cdot\Big[\begin{array}{c}\cos\\ \sin\end{array}(\gamma_0\xi\sec\theta)\cdot \cos(\gamma_0\bar{b}\varphi(\xi)\sec\theta\tan\theta)\frac{d\varphi}{d\xi} \mp \frac{\sin}{\cos}(\gamma_0\xi\sec\theta)\Big\{\bar{b}\tan\theta\sin(\gamma_0\bar{b}\varphi(\xi)\sec\theta\tan\theta)\left(\frac{d\varphi}{d\xi}\right)^2 - \frac{1}{\gamma_0}\cos\theta\cos(\gamma_0\bar{b}\varphi(\xi)\cdot\sec\theta\tan\theta)\frac{d^2\varphi}{d\xi^2}\Big\}\Big]d\xi \tag{3.15}
$$

The optimization becomes more stable by the employment of eq. (3.15), because the exact evaluation of $d\chi/d\xi$ is not so easy for the near field of bow and stern.

Since the objective function must be evaluated as quickly as possible in spite of its complexity, we need the high speed calculations with regard to the fluid velocities in eq. (3.14). To calculate these values, both the exact scheme given by Hess & Smith[11] and the approximate scheme shown in the appendix are used properly according to the prescribed rules.

Fig. 6 shows the examples to check up the fairness effects based on the formulation (2) stated in 3.1. Fairing constraint plays a role obtaining stable optimum shapes. In Fig. 7, the examples based on the low speed theory are compared with that based on the thin ship theory shown in Fig. 1. In Fig. 8, optimum coefficients of fineness are compared with results based on various methods such as the minimum wave resistance form by Maruo and Bessho[3], the optimum shape of slender ships by Maruo[12], Yamagata's results[13] based on Taylor standard series and the results by means of SUMT based on the thin ship theory given in the preceding section. The present results show a similar tendency to that of Taylor standard series.

4. Hull Form Improvement of Practical Ships

4.1 Statement of the Problem

Results of the minimum wave resistance problem shown in the preceding chapter may be useful to the determination of the sectional area curve in the preliminary design stage. In a practical sence, however, the method of hull form improvement by distorting lines from a given hull form of arbitrary frame lines is also useful. The main purpose of this section is to discuss the common statements of the present techniques about the hull form improvement by means of SUMT. A similar investigation by means of Feasible Direction Method was carried out by Amromin et al.[14] But SUMT has the advantage that any constraints can be added in a comparatively easy way.

For this kind of the problem, it is generally assumed that the principal particulars L(length), B(breadth), T(draught), the design speed U and the offset table of the initial hull form are given. In the present work, only the fore body shape is improved so as to make the objective function minimum under the basic design constraints, and the after body shape is fixed in the initial form.

The present formulation is also specified according to the right hand co–ordinate system used in the preceding problem. Co–ordinates x, y and z are normalized as follows in this place,

$$x=l\xi,\quad y=B/2\cdot\eta,\quad z=T\zeta \tag{4.1}$$

where l is the half length $L/2$. Then the equation of the hull surface is expressed as

$$\eta=\eta(\xi,\zeta). \tag{4.2}$$

The following 3 types of formulation are introduced and studied in the present work.

(1) Application of the thin ship theory
(2) Application of the low speed theory
(3) Application of the wave analysis

The general form of the objective function is defined such as

$$I=\alpha I_W+\beta I_F,\quad I_W=I_M \text{ or } I_L \tag{4.3}$$

where I_M being wave resistance by the thin ship theory (case(1)), I_L being also wave resistance by the low speed theory (case(2)), I_F being plank friction, and α, β being suitable weighting factors. The functional I_M or I_L is written as follows,

$$\left.\begin{aligned}\left.\begin{matrix}I_M\\ I_L\end{matrix}\right\}=\frac{\rho U^2L^2\gamma_0{}^2t^2b^2}{\pi}\int_0^{\pi/2}(\{p(\theta)\}^2\\ +\{q(\theta)\}^2)\sec^3\theta\, d\theta\end{aligned}\right\} \tag{4.4}$$

where $b=B/L$, $t=T/l$, $\gamma_0=gl/U^2=1/2\,Fn^2$. Amplitude functions $p(\theta)$, $q(\theta)$ have different expressions in each theory. In the case (3), however, the objective function is slightly modified. Detailed informations of these are given in later sections. When the coefficient of the plank friction C_f is given, we can write I_F as follows,

$$I_F=\frac{1}{2}\rho U^2 C_f S \tag{4.5}$$

$$\left.\begin{aligned}S=LT\iint_{Sc}\\ \sqrt{1+b^2\left(\frac{\partial\eta}{\partial\xi}\right)^2+\left(\frac{b}{t}\right)^2\left(\frac{\partial\eta}{\partial\zeta}\right)^2}\cdot\end{aligned}\right\} \tag{4.6}$$

$$d\xi d\zeta+\frac{1}{2}BL\int_{-1}^{1}\eta(\xi,1)d\xi$$

where S and S_c indicate the wetted hull surface area and the ship center plane ($\eta=0$) respectively. In this work, the plank friction is evaluated by the Schoenherr's mean line.

The objective function (4.3) corresponds to the total resistance, and the weighting factors are introduced in order to improve its estimation. We can select α and β as follows,

$$\alpha=R_{WO}/I_{WO},\quad \beta=1+K_0 \tag{4.7}$$

where R_{WO}, I_{WO} and K_0 mean the measured (or estimated) wave resistance, the theoretical wave resistance and the form factor respectively, all of which are the values for the initial hull form. When we use the weighting factors determined from eq. (4.7), the calculated value of the objective function for the initial hull form becomes identical with the measured total resistance. In the numerical examples shown in subsequent sections, the weighting factors are selected by the present procedures.

4.2 Hull Surface Approximation and Design Constraints

The major part of the conventional hull surface is smooth. In this paper, however, for the sake of simplified computation, it is assumed that the hull surface is approximated by the polyhedron formed by triangular panels with nodal points at intersections of Square Stations (S.S.) and Water Lines (W.L.) as an example shown in Fig. 9. In the after part of the hull, the diagonal lines are taken in opposite directions in order to correspond to a general tendency of bow and buttock lines, but its shape is being fixed as described in the statement of the problem. According to this approximation, several computations about the objective function can be simplified and executed rapidly in the optimization process, because $\partial\eta/\partial\xi$ and $\partial\eta/\partial\zeta$ become constant on each panel. The outline of the computation procedures about the objective function is explained in later sections. Computations of the wetted hull surface area and other particulars can be also simplified.

When S. S. and W. L.are expressed by $\xi=\xi_i$ ($i=1, 2, \ldots\ldots, I$: for fore part) and $\zeta=\zeta_j$ ($j=1, 2, \ldots\ldots, J$), we can take directly the ordinates $\eta(\xi_i, \zeta_j)=\eta_{ij}$ as the design variables. These variables must be transformed and stored as a vector form (one dimensional array) in the actual optimization program. In our formulation of the problem, the basic design constraints must be specified by these design variables. In this study, the following relations are employed as the basic constraints.

$$\left.\begin{array}{ll}
1)\ \eta_{ij}\geqq 0 & 2)\ \eta_{ij}\geqq\eta_{i+1,j}\\
3)\ \eta_{ij}\geqq\eta_{i,j+1} & \\
4)\ \dfrac{\eta_{ij}-\eta_{i-1,j}}{\xi_i-\xi_{i-1}}\gtrless\dfrac{\eta_{i+1,j}-\eta_{ij}}{\xi_{i+1}-\xi_i} & \\
5)\ \dfrac{\eta_{ij}-\eta_{i,j-1}}{\zeta_j-\zeta_{j-1}}\gtrless\dfrac{\eta_{i,j+1}-\eta_{ij}}{\zeta_{j+1}-\zeta_j} & \\
6)\ \Delta\geqq\Delta_0 & \\
7)\ \Delta_B\leqq(1+\delta)\Delta_{B0},\ \delta>0 &
\end{array}\right\} \tag{4.8}$$

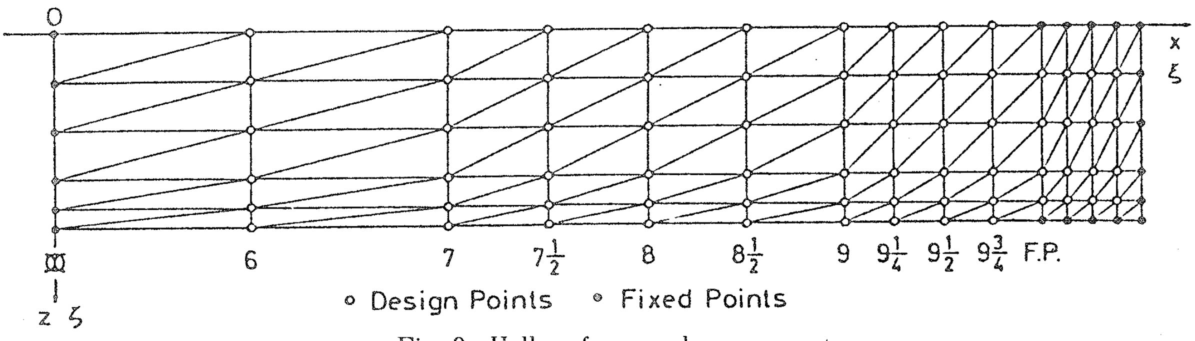

Fig. 9 Hull surface panel arrangement

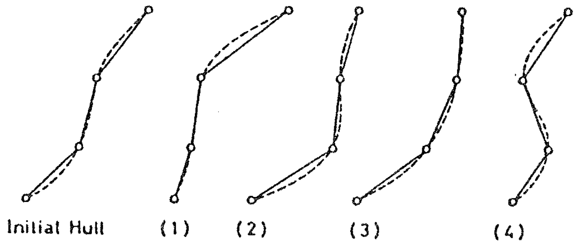

Fig. 10 Variation of frame lines

The constraints 1), 2) and 3) are introduced from the geometrical point of view. Tendencies of waterlines and frame lines of the initial hull form are kept by the constraints 4) and 5), in which directions of inequality are determined from the initial offset check in the optimization program. For example, Fig. 10 shows several types of variation of frame lines. In this figure, the initial frame line can vary as the type (1) or (2), however the type (3) or (4) is rejected by the employment of constraint 5). In the practical optimization, 3), 4) and 5) are additioned to the suitable S.S. determined from the intuitive consideration of initial lines. In 6), Δ and Δ_0 indicate the displacement excluding protruded bulb of the improved hull and the initial hull respectively. The final constraint 7), in which Δ_B and Δ_{B0} indicate the displacement of protruded bulb of the improved hull and the initial hull respectively, is optionally additioned in the problem if necessary.

4.3 Numerical Examples

4.3.1 Application of the Thin Ship Theory

When applying the thin ship theory to the present problem, the amplitude functions in eq. (4.4) are given as follows.

$$\left.\begin{aligned} &\left.\begin{matrix} p(\theta) \\ q(\theta) \end{matrix}\right\} = -\iint_{Sc} \frac{\partial \eta}{\partial \xi} \begin{matrix} \cos \\ \sin \end{matrix} \\ &\qquad (\gamma_0 \xi \sec\theta)\, e^{-\gamma_0 t \zeta \sec^2\theta}\, d\xi\, d\zeta \end{aligned}\right\} \quad (4.9)$$

The numerical evaluations of these integrals are carried out without difficulty, because $\partial \eta / \partial \xi$ becomes a constant on each triangular panel by means of the approximation in the preceding section.

In this chapter, two initial hull forms are employed as the bases of numerical examples. One is Series 60, $C_b=0.6$ model[15] and the other is SR138 container ship model.[16] Particulars of these are as follows, where L_B is the length of protruded bulb.

(1) Series 60 model
$L=121.92$m, $B=16.25$m, $T=6.50$m, $C_b=0.6$, $L.C.B.=1.4$% aft,
$\Delta_0=7{,}924$ ton, $L_B/L=0$

(2) SR 138 model
$L=195.0$m, $B=30.0$m, $T=10.5$m, $C_b=0.5716$, $L.C.B.=1.6$% aft,
$\Delta=35{,}987$ ton, $\Delta_{B0}=20$ ton, $L_B/L=0.01$

The respective fore body shapes under L. W. L. are shown in Fig. 11 and 12.

Examples of the improved fore body shapes are shown in Fig. 13～16 for series 60 (Model NP1, NP2, NP4, NP5) and in Fig. 17～19 for SR138 (Model NP6, NP7, NP8). Optional constraint 7) in eq. (4.8) is not taken into account except Model NP7 and NP8. In case of Model NP7 and NP8, the constraint 7) with $\delta=0.5$ is employed. The other design conditions about the design Froude number etc. are specified under respective figures. Theoretical reductions of the objective function are about 20% in Model NP1, NP2, about 12% in Model NP4, NP5 and about 7% in Model NP6, NP7, NP8.

In case of Model NP1, NP2 and NP6, large deformations of frame lines are observed near the bow. These results have relations with the design speed, because they are designed at the hump of theoretical curve of wave resistance of the initial hull form. The displacement of protruded part of the bulb in Model NP7 is suppressed in comparison with that of Model NP6 on account of the consideration of the optional constraint.

Since the improved hull form lacks in smoothness in general because of the present hull surface approximation, the fairing operations are needed for the practical application. The fairing problem of hull surface is important but difficult in itself, hence it is not taken into consideration at present.

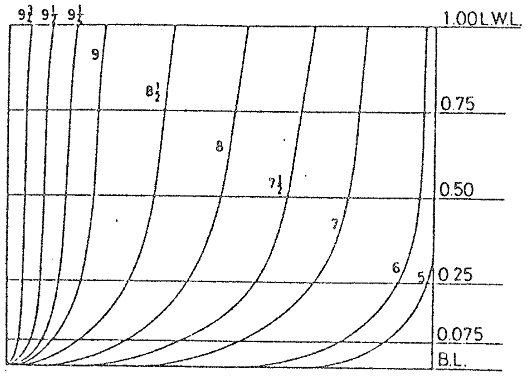

Fig. 11 Initial hull form : Series 60, $C_b=0.6$ (Model SER60)

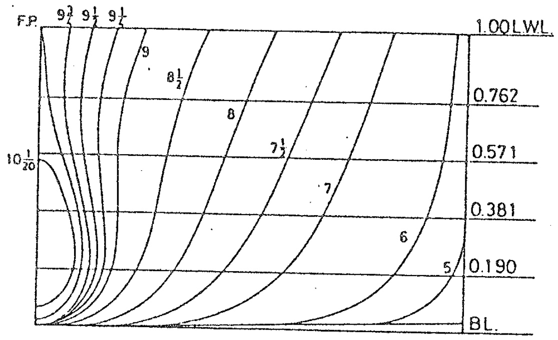

Fig. 12 Initial hull form : SR138

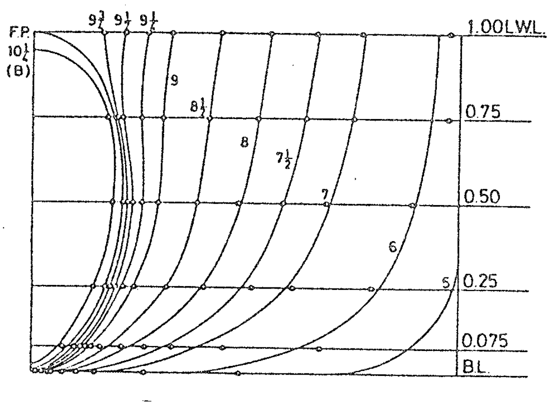

Fig. 13 Example for Series 60 (Model NP1 : Fn = 0.286, $\alpha=0.414$, $\beta=1.2$, $L_B/L=0.05$)

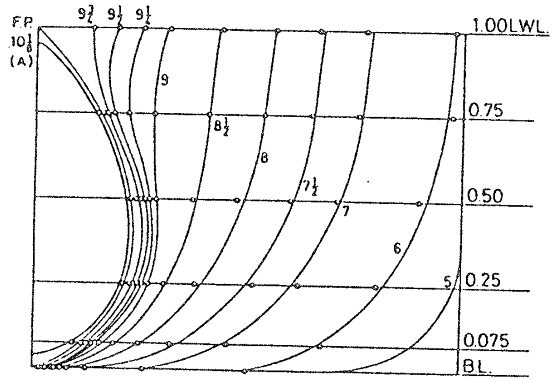

Fig. 14 Example for Series 60 (Model NP2 : Fn = 0.286, $\alpha=0.414$, $\beta=1.2$, $L_B/L=0.025$)

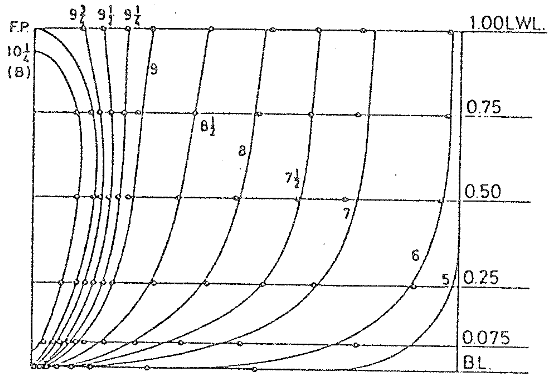

Fig. 15 Example for Series 60 (Model NP4 : Fn = 0.325, $\alpha=0.938$, $\beta=1.2$, $L_B/L=0.05$)

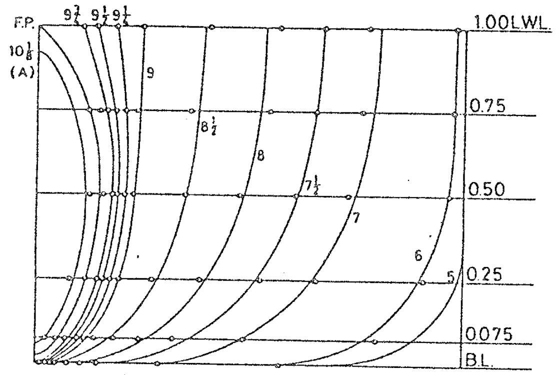

Fig. 16 Example for Series 60 (Model NP5 : Fn = 0.325, $\alpha=0.938$, $\beta=1.2$, $L_B/L=0.025$)

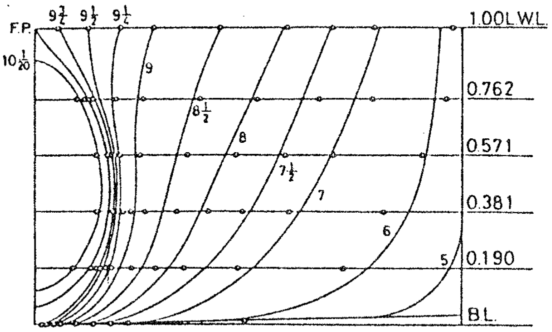

Fig. 17 Example for SR138 (Model NP6 : Fn=0.270, α=0.334, β=1.2, L_B/L=0.01)

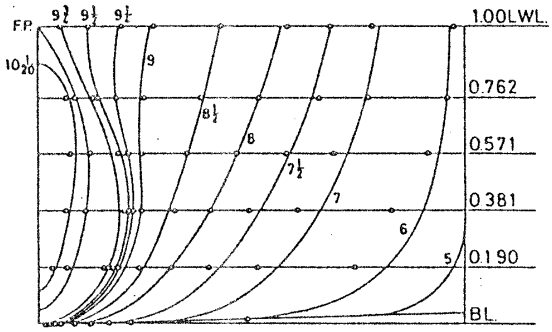

Fig. 18 Example for SR138 (Model NP7 : Fn=0.270, α=0.334, β=1.2, L_B/L=0.01, with constraint 7))

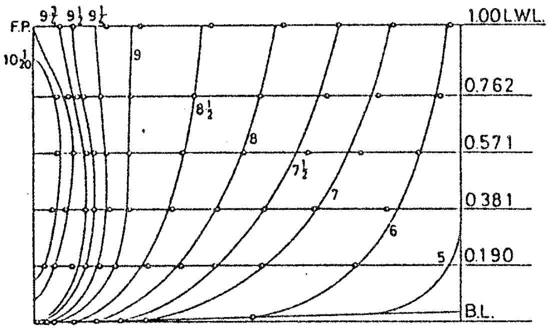

Fig. 19 Example for SR138 (Model NP8 : Fn=0.255, α=0.460, β=1.2, L_B/L=0.01, with constraint 7))

4.3.2 Application of the Low Speed Theory

In place of the thin ship theory, the application of the low speed theory to the hull form improvement is discussed here. The simplified formula is used in 3. 3. 2, however in the present problem, the optimization based on the rigorous expressions of the amplitude function given by Maruo[17] is tried ; that is

$$
\left.\begin{aligned}
\left.\begin{matrix} p(\theta) \\ q(\theta) \end{matrix}\right\} = & -\frac{2\pi}{bt}\iint_S \sigma(\xi,\eta,\zeta)\begin{matrix}\cos\\ \sin\end{matrix}\left\{\gamma_0 \sec\theta(\xi+b\eta\tan\theta)\right\}e^{-\gamma_0 t\zeta\sec^2\theta}\,dS \\
& +\frac{2\pi}{\gamma_0 t}\int_C \sigma(\xi,\eta,0)\begin{matrix}\cos\\ \sin\end{matrix}\left\{\gamma_0 \sec\theta(\xi+b\eta\tan\theta)\right\}n_0\,d\eta \\
& -\frac{1}{2\gamma_0 t}\iint_F \Phi(\xi,\eta)\begin{matrix}\cos\\ \sin\end{matrix}\left\{\gamma_0 \sec\theta(\xi+b\eta\tan\theta)\right\}d\xi\,d\eta \\
& +\frac{1}{2\gamma_0 t}\iint_W \Psi(\xi,\eta)\begin{matrix}\cos\\ \sin\end{matrix}\left\{\gamma_0 \sec\theta(\xi+b\eta\tan\theta)\right\}d\xi\,d\eta
\end{aligned}\right\} \quad (4.10)
$$

with

$$
\left.\begin{aligned}
\Phi(\xi,\eta) = & \frac{1}{2}\left\{\left(-2\frac{\partial}{\partial\xi}+u\frac{\partial}{\partial\xi}+v\frac{1}{b}\frac{\partial}{\partial\eta}\right)(u^2+v^2)\right. \\
& \left.-\frac{1}{t}\frac{\partial w}{\partial\zeta}(-2u+u^2+v^2)\right\}\text{on } F, \\
\Psi(\xi,\eta) = & \frac{\partial u}{\partial\xi}\ \text{on } W.
\end{aligned}\right\} \quad (4.11)
$$

In these expressions, S, C, F and W denote the wetted hull surface, the waterline, the undisturbed free surface and the water plane respectively, and n_0 is the direction cosine of the outward normal to S with respect to x-axis. The source density σ and fluid velocities u, v and w, all of which are normalized by U, are obtained from the perturbation velocity potential around the double model. Since the objective function is fully nonlinear about the design variables as shown in the above expression, the

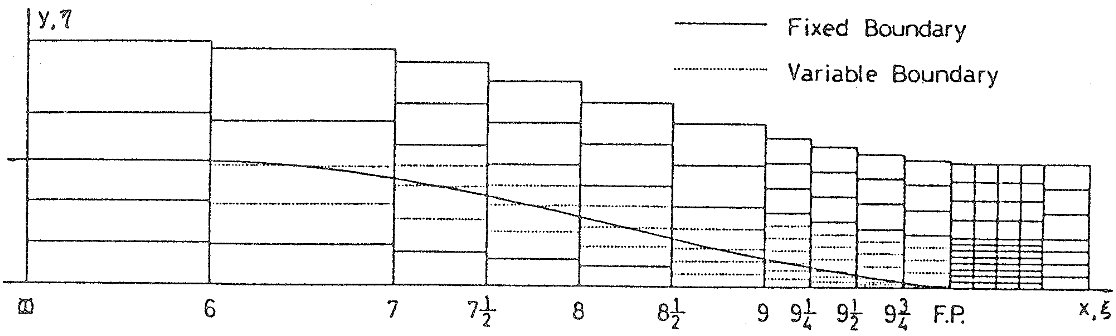

Fig. 20 Panel arrangement of free surface and water plane

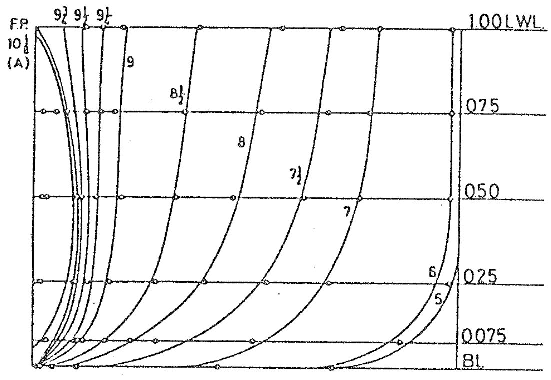

Fig. 21 Example for Series 60 (Model NP3 : Fn= 0.286, α=0.827, β=1.2, L_B/L=0.025).

optimization by means of the variational method is hopeless.

In order to calculate the objective function as rapidly as possible, ideas similar to those shown in 3. 3. 2 are also introduced in the present optimization. The evaluation of the source density are carried out by the method of Hess & Smith or the approximate method given in the appendix. Either of the two is selected in the optimization program in accordance with the prescribed rules. Together with the division of S, we must divide F and W as in Fig. 20. The panels near the waterline are rearranged with the deformation of the hull in the optimization process. Both the exact scheme and the approximate scheme are also provided to evaluate Φ and Ψ.

An example based on the low speed theory is shown in Fig. 21 (Model NP3) for Series 60. In this case, about 8% reduction of the objective function is attained. The obtained bulb size is smaller than that of Model NP1 or NP2 based on the thin ship theory, and the frame lines before F.P. become unstable. Then the protruded length of bulb of Model NP3 is cut at $L_B/L=0.025$, though the optimization is executed as $L_B/L=0.05$. Generally speaking, CPU time is about 10 to 15 times greater than that based on the thin ship theory.

4.3.3 Application of the Wave Analysis

The method of wave analysis proposed by Newman[18] and Sharma[19] and established by Ikehata[20] et. al comes into practical use at present. One of the merit of this technique is that the free wave spectrum for respective hull forms is determined experimentally. As the free wave spectrum contains many informations with respect to the wave making phenomena,we can make use of the result of wave analysis to the hull form design in many ways.[21)22)23]

In order to use the wave analysis of the initial hull form, the objective function defined by eq. (4.3) and (4.4) is slightly modified as

$$I=I_{WP}+\beta I_F \tag{4.12}$$

$$\left.\begin{aligned} I_{WP}=&\frac{\rho U^2 L^2 \gamma_0{}^2 t^2 b^2}{\pi}\int_0^{\pi/2} w(\theta)\cdot \\ &(\{p(\theta)\}^2+\{q(\theta)\}^2)\sec^3\theta\, d\theta \end{aligned}\right\} \tag{4.13}$$

where the amplitude functions are defined by eq. (4.9). In eq. (4.13), $w(\theta)$ means the weighting function and we assume the following polynomial expression.

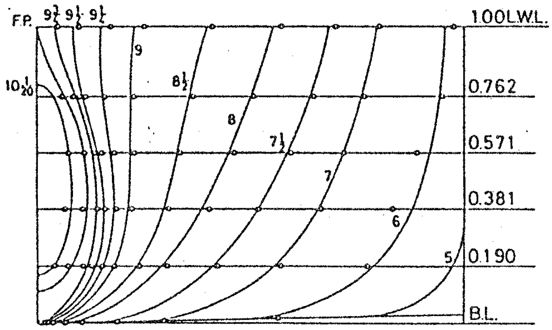

Fig. 22 Example for SR138 (Model NP9 : Fn=0.270, $\alpha=0.0395$, $\lambda_1=0.2179$, $\beta=1.25$, $L_B/L=0.01$)

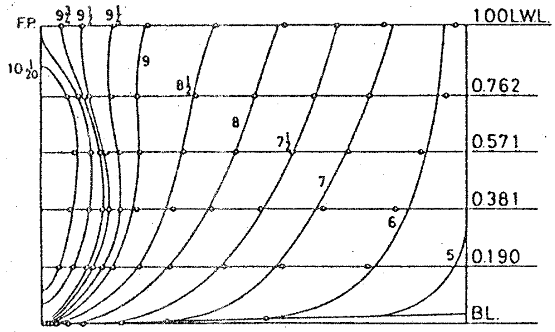

Fig. 23 Example for SR138 (Model NP10 : Fn=0.270, $\alpha=0.0754$, $\lambda_1=0.0315$, $\lambda_2=0.1593$, $\beta=1.25$, $L_B/L=0.01$)

$$w(\theta)=\alpha+\sum_{n=1}^{N}\lambda_n\theta^n \tag{4.14}$$

If we select the coefficients as $\lambda_n=0$, the problem is equal to 4.3.1. These coefficients are determined from the concept of equivalence such as

$$\left.\begin{aligned}&\int_0^{\pi/2} w(\theta)(\{p(\theta)\}^2\\&\quad+\{q(\theta)\}^2)\sec^3\theta\, d\theta\\&=\int_0^{\pi/2}(\{p_E(\theta)\}^2\\&\quad+\{q_E(\theta)\}^2)\sec^3\theta\, d\theta\end{aligned}\right\} \tag{4.15}$$

with respect to the initial hull form, where $p_E(\theta)$, $q_E(\theta)$ denote the amplitude functions determined from the results of wave analysis.

The numerical examples are provided for SR138 as shown in Fig. 22, 23 (Model NP9, NP10). For these examples, the following weighting functions which satisfy the condition (4.15) are employed.

$$w(\theta)=0.0395+0.2179\theta \quad \text{for Model NP9}$$

$$w(\theta)=0.0754+0.0315\theta+0.1593\theta^2 \quad \text{for Model NP10}$$

The obtained bulb shapes are more acceptable than those of Model NP6 and NP7 based on the method of 4.3.1 from the practical point of view.

4.4 Experimental Verification

In order to verify the present method of hull form improvement, model tests involving the towing test and the wave pattern analysis are carried out. Test results about the Series 60 (SER60) model and its improved hull forms (NP1～5) are shown in Fig. 24, 25, and those about the SR138 model and its improved hull forms (NP6～10) are shown in Fig. 26, 27, where C_r means the residuary resistance coefficient based on the towing test and C_{wp} means the wave pattern resistance coefficient analyzed by the logitudinal cut method.

All improved hull forms have attained the resistance reduction at their design speeds as compared with the result for each initial hull form. In many cases, the small hollow is observed on the curve of resistance coefficient near the respective design points.

In Fig. 24,the models NP1 and NP2 with large bulbs designed by the thin ship theory show greater reduction than that of NP3 designed by the low speed theory. In consequence of the present work, it seems that we had better choose the thin ship theory from the points of view of computer time and resistance reduction.

In comparison with Fig. 26 and Fig. 27, the performance of NP9 and NP10 are superior. The utilization of the result of wave analysis seems very efficient in the present techniques of hull form improvement.

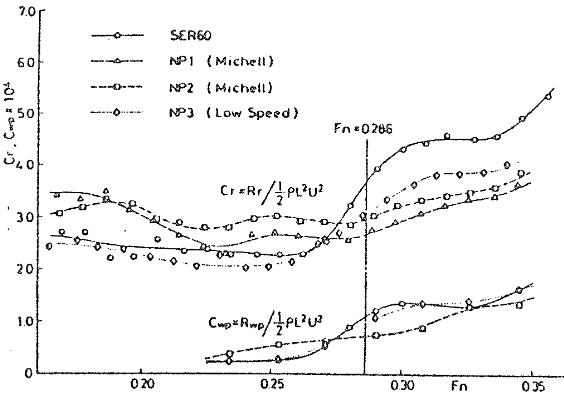

Fig. 24 Residuary and wave pattern resistance coefficients

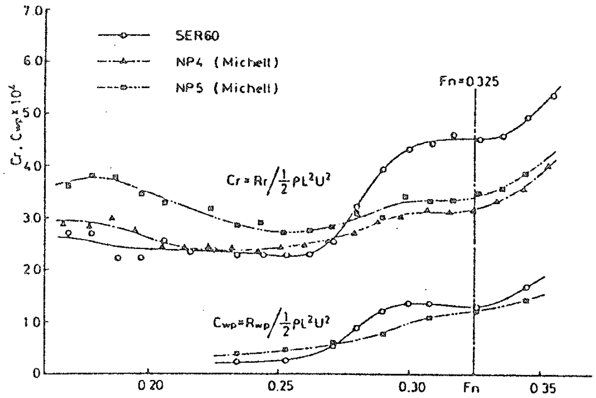

Fig. 25 Residuary and wave pattern resistance coefficients

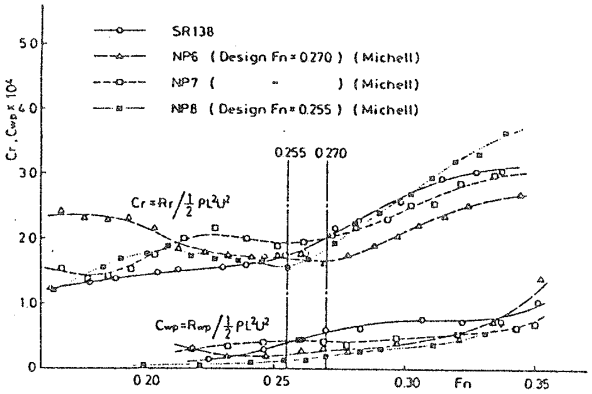

Fig. 26 Residuary and wave pattern resistance coefficients

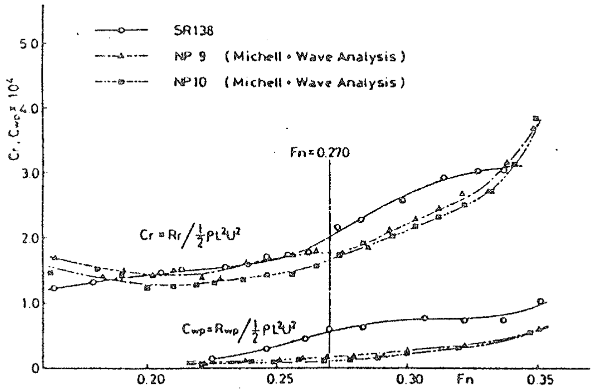

Fig. 27 Residuary and wave pattern resistance coefficients

5. Concluding Remarks

In the present study, two types of the hull form design problem are discussed by means of the nonlinear programming. One is the minimization of wave resistance of wall–sided ships and the other is the improvement of practical hull forms in order to reduce the total resistance.

In the former problem, the thin ship theory and the low speed theory are applied, and several numerical solutions are shown as examples. By the employment of the thin ship theory, optimum sectional area curves with three types of ending, i.e. normal, bluff and bulbous, can be obtained. The optimum solutions can be determined by means of the present method also in the case of low speed theory in spite of its extreme nonlinearity.

For the problem of hull form improvement, both the thin ship theory and the low speed theory are also applied. In addition to these, the present technique has been revised by the application of wave analysis. These improvement technique have been appraised by model tests based on the towing test and the wave pattern analysis, and their usefulness is confirmed. The nonlinear programming technique provides a rational method for the determination of lines of practical hull forms.

As a future work, we have to extend the present technique to wider aspects of hull form design, namely, the optimization of total propulsive performance including the interaction of hull, propeller and rudder.

Acknowledgement

The author wish to express his deep appreciation to Prof. H. Maruo, Prof. M. Ikehata and Prof. M. Higuchi of Yokohama National University for their helpful suggestions and encouragement. The numerical work has been carried out by the aid of HITAC M−280H/M−200H of Computer Center of University of Tokyo.

References

1) Kowalik, J. and Osborn, M.R. : METHOD FOR CONSTRAINED OPTIMIZATION PROBLEMS, Elsevier, (1968).
2) Zangwill, W.I. : Minimizing a Function without Calculating Derivatives, Computer Journal, Vol. 10, (1967).
3) Maruo, H. and Bessho, M. : Ships of Minimum Resistance, Selected Papers from JSNA of Japan, Vol. 3, (1969).
4) Maruo, H. and Yamakoshi, Y. : Calculation of the Ship Form of Minimum Wave−Resistance with Finite Draft, JSNA of Japan, vol. 130, (1971), (in Japanese).
5) Maruo, H., Kasahara, K. and Miyazawa, M. : Ship Forms of Minimum Wave Resistance with Bulbs, JSNA of Japan, vol. 135, (1974), (in Japanese).
6) Maruo, H., Kasahara, K., Suzuki K. and Kawamura T. : On the Ship Form of Minimum Wave Resistance with a Bow Bulb, JSNA of Japan, Vol.138, (1975), (in Japanese).
7) Suzuki, K. : Studies on the Application of Nonlinear Programming to Hull Form Design Based on Wave Resistance Theory, Doctoral Thesis, Osaka University, (1985), (in Japanese).
8) Baba, E. and Takekuma, K. : A Study on Free Surface Flow around Bow of Slowly Moving Full Forms, JSNA of Japan, Vol. 137, (1975).
9) Maruo, H. : Wave Resistance of a Ship with Finite Beam at Low Froude Numbers, Bulletin of the Faculty of Engg., Yokohama Nat. Univ., Vol. 26, (1976).
10) Maruo, H. and Suzuki K. : Wave Resistance of a Ship of Finite Beam Predicted by the Low Speed Theory, JSNA of Japan, Vol. 142, (1977).
11) Hess, J. L. and Smith, A.M.O. : Calculation of Nonlifting Potential Flow about Arbitrary Three −Dimensional Bodies, JSR, Vol. 8, No. 2, (1964).
12) Maruo, H. : Calculation of the Wave Resistance of Ships, the Draught of Which is as Small as the Beam, JSNA of Japan, Vol. 112, (1962).
13) Yamagata, M. : *Senkeigaku*, Vol. 1, Tennensha, (1941), (in Japanese).
14) Amromin, E.L. and Timoshin, Yu. S. : Determination of Minimum Resistance Hull Forms by Methods of Nonlinear Programming, Int. Seminar on Wave Resistance, Tokyo, SNA of Japan, (1976).
15) Todd, F.H. : Some Further Experiments on Single−Screw Marchant Ship Forms−Series 60, Trans. of SNAME, Vol. 61, (1953).
16) SR138 Report, The Shipbuilding Research Association of Japan, No. 183, (1973), (in Japanese).
17) Maruo, H. and Suzuki, K. : Computation of Wave Resistance by Means of the Low Speed Theory, Workshop on Ship Wave−Resistance Computations, Washington, DTNSRDC, (1979).
18) Newman, J. N. : The Determination of Wave Resistance from Wave Measurements along a Parallel Cut, Int. Seminar on Wave Resistance, Ann Arbor, (1963).
19) Sharma, S.D. : A Comparison of the Calculated and Measured Free−Wave Spectrum of an Inuid in Steady Motion, Int. Seminar on Wave Resistance, Ann Arbor, (1963).
20) Ikehata, M. : On Experimental Determination of Wave−Making Resistance of a Ship, Japan Shipbuilding & Marine Engineering, Vol. 4, No. 5, (1969).
21) Baba, E. : An Application of Wave Pattern Analysis to Ship Form Improvement, JSNA of Japan, Vol. 132, (1972).
22) Ogiwara, S. : Study on the Application of Wave Pattern Analysis to the Tank Test with Ship Models, IHI Engg. Review, Vol. 8, (1975).
23) Tsutsumi, T. : An Application of Wave Resistance Theory to Hull Form Design,

JSNA of Japan, Vol. 144, (1978).

Appendix

The hull surface S^* and S which are slightly different each other are considered. When we assume that the flow field around the double model of S^* is calculated by the Hess & Smith method,[11] the values on S^* are known quantities. The object of this article is to calculate the flow around the double model of S approximately by using the known values on S^*.

The surface S is generally divided by N quadrilateral elements in order to apply Hess & Smith method. Using the discretization procedures by Hess & Smith, the source density σ_i and the fluid velocities u_i, v_i and w_i on i–th element are written as

$$\left.\begin{aligned}\sigma_i=-\frac{1}{2\pi}\Bigl\{&\Bigl(-U+\sum_{j\neq i}A_{ij}\ \sigma_j\Bigr)n_x\\ &+\Bigl(\sum_{j\neq i}B_{ij}\ \sigma_j\Bigr)n_y+\Bigl(\sum_{j\neq i}C_{ij}\,\sigma_j\Bigr)n_z\Bigr\}\end{aligned}\right\}\quad(\mathrm{A}.1)$$

$$\left.\begin{aligned}u_i&=2\pi n_x\sigma_i+\sum_{j\neq i}A_{ij}\ \sigma_j\\ u_i&=2\pi n_y\sigma_i+\sum_{j\neq i}B_{ij}\ \sigma_j\\ w_i&=2\pi n_z\sigma_i+\sum_{j\neq i}C_{ij}\ \sigma_j\end{aligned}\right\}\quad(\mathrm{A}.2)$$

where n_x, n_y, n_z are the direction cosines of the outward normal on i–th element. In the optimization process , we want to estimate the source density and the fluid velocities without calculating the influence coefficients A_{ij}, B_{ij}, C_{ij} for the purpose of the high speed evaluation of the objective function. In the first place, the approximate scheme for the source density can be obtained by replacing σ_j, A_{ij}, B_{ij}, C_{ij} of right hand side of eq. (A.1) by known values σ_j^*, A_{ij}^*, B_{ij}^*, C_{ij}^* on S^*. Inserting these approximate values σ_i and σ_j into eq. (A.2) and replacing A_{ij}, B_{ij}, C_{ij} by A_{ij}^*, B_{ij}^*, C_{ij}^*, the fluid velocities are evaluated approximately. The accuracy of the present numerical scheme is discussed in the reference 7).